

Hubble Space Telescope Imaging of Bipolar Nuclear Shells in the Disturbed Virgo Cluster Galaxy NGC 4438¹

Jeffrey D. P. Kenney² & Elizabeth E. Yale²

kenney@astro.yale.edu, eey2@astro.yale.edu

ABSTRACT

We present broadband and narrowband *Hubble Space Telescope* images of the central region of the heavily disturbed Virgo cluster galaxy NGC 4438 (Arp120), whose nucleus has been described as a type 1 LINER or dwarf Seyfert. Narrowband H α and [NII] HST images reveal striking bipolar shell features, 1 kpc in projected length from end-to-end, which are likely the result of an outflow from the nuclear region experiencing a strong interaction with the ISM. While these outflow shells share similarities with those in some other starburst or AGN galaxies, these in NGC 4438 are notable because NGC 4438 harbors neither a luminous circumnuclear starburst nor a luminous AGN.

The shells appear to be closed at their outer ends, suggesting that the outflow in NGC 4438 is dynamically younger than those in some other galaxies. The radio continuum emission is strongly enhanced near the outer ends of the shells, suggesting working surfaces arising from collimated nuclear outflows which have impacted and shocked the surrounding ISM. The 2 shells are quite different, as the northwestern (NW) shell is luminous and compact, while the southeastern (SE) shell is 2.5 times longer and much fainter, in both optical emission lines and the non-thermal radio continuum. The differences between the 2 shells may be attributed to a difference in ISM density on the 2 sides of the nuclear disk. Such an ISM asymmetry exists on larger scales in this heavily disturbed galaxy.

At the base of the outflow is a nuclear source, which is the highest surface brightness source in the galaxy at optical wavelengths. This source is resolved with a FWHM=0.3''=25 pc and has modest luminosities, uncorrected for extinction, of 5×10^{38} erg s $^{-1}$ in H α , and $M_B=-13$. We discuss whether the outflow is powered by a low luminosity AGN or a compact nuclear starburst. The kinetic energy associated with the ionized gas in the shells is $\sim 10^{53}$ ergs, which could be produced either by massive star formation or an AGN. While the NW shell,

²Yale University Astronomy Department, P.O. Box 208101, New Haven, CT 06520-8101

which contributes most of the flux in most ground-based apertures centered on the nucleus, exhibits LINER-type line ratios, the nucleus has an $\text{H}\alpha/[\text{NII}]$ ratio consistent with an HII region. Although there appears to be very little massive star formation occurring in the central kpc, the nucleus may contain a partially obscured, young nuclear star cluster. On the other hand, the collimation of the southeastern shell, and the strongly enhanced radio continuum emission at the outer ends of the shells are more easily explained by jets associated with a nuclear black hole than a compact nuclear starburst, although there is no direct evidence of a jet. The 2000 km s^{-1} broad line component could be due to an AGN broad line region but might also be due to high velocity gas in the outflow. Since NGC 4438 has a large bulge, a large nuclear black hole might be expected.

Subject headings: galaxies: active — galaxies: clusters: individual (Virgo) — galaxies: interactions — galaxies: ISM — galaxies: jets — galaxies: nuclei — galaxies: peculiar

1. Introduction

The nuclei of galaxies exhibit an enormous range of activity, and the factors which govern their differences are far from understood. LINERs (low ionization nuclear emission regions), which are among the most common type of galactic nucleus, are clearly a heterogeneous group of objects, and different galaxies likely have different origins for the excitation of ionized gas whose spectra lead to the LINER classification. The excitation mechanisms include photoionization from low luminosity AGN, photoionization from hot stars, and shocks from AGN jets or starburst outflows (for a review see Filippenko 1996). Progress towards understanding the nature of LINERs must involve high resolution studies of nearby nuclei with a wide range of properties. In this paper we focus on one nearby galaxy whose nucleus, classified variously as a LINER 1 or a 'dwarf Seyfert' (due to its nuclear broad line component), can reveal some of the physical processes which occur in galactic nuclei.

NGC 4438 (Arp 120) is a highly inclined and very peculiar large spiral galaxy near the center of the Virgo Cluster ($D=16 \text{ Mpc}$). Its disturbed stellar distribution indicates that it recently experienced some type of major gravitational encounter (Combes et al. 1988; Moore et al. 1996; Katsiyannis et al. 1998). Its complex and strongly disturbed ISM (Kotanyi et

¹Based on observations with the *Hubble Space Telescope* which is operated by AURA, Inc., under NASA contract NAS 5-26555

al. 1983; Warmels 1988; Cayatte et al. 1990; Keel & Wehrle 1993; Kenney et al. 1995) is quite different from that of any other galaxy presently known, and it is likely that a high-velocity ISM-ISM collision (Kenney et al. 1995) and/or an ICM-ISM interaction (Kotanyi et al. 1983; Keel & Wehrle 1993) is responsible for the ISM disturbance. While the origin of the disturbance is not a focus of the present paper, it is relevant that much of the ISM is significantly displaced to the west of the galaxy’s main disk. The galaxy disturbance may well be responsible for some of the properties of the nuclear region.

The nuclear region of NGC 4438 has a complex and unusual radio continuum morphology which has not previously been understood (Hummel & Saikia 1991; Keel & Wehrle 1993). The optical “nucleus?” of NGC 4438 has been classified as a LINER (Heckman 1980; Stauffer 1982; Keel 1983), but as shown here, the source with LINER-type line ratios is not the real nucleus. The detection of high-velocity gas suggests that the nucleus is ‘active’. Ho et al. (1997) find a weak broad component in the H α line whose FWHM is 2050 km s $^{-1}$, making NGC 4438 a “dwarf Seyfert”, or LINER 1.9 nucleus.

In this paper, we present and discuss the results of HST imaging of the central region of NGC 4438, which reveal asymmetric bipolar shell features strongly suggestive of outflow from the nucleus. The dominant source of both optical line and radio continuum emission in the central few arcseconds (i.e. at ground-based resolution) of NGC 4438 is not the nucleus itself, but emission from an outflow which is experiencing a strong interaction with the surrounding ISM. We also detect a compact nuclear source (FWHM= 0.3’’), which does not have LINER-type line ratios, but instead has an H α /[N II] ratio similar to an HII region. We discuss whether the nuclear outflow is powered by a compact nuclear starburst or by jets from a low luminosity AGN.

2. Observations

WFPC2 images of NGC4438 were obtained in March 1999 with broadband F450W (B), F675W (R) and F814W (I) and narrowband F656N and F658N filters. The bandpasses of F656N and F658N cover the λ 6563Å H α and the λ 6583Å [N II] lines, respectively, and are narrow enough (22.0 and 28.5 Å) to separate these nearby lines. Since NGC 4438 has a redshift of only 71 km s $^{-1}$ (Kenney et al. 1995), these emission lines fall within the bandpasses of these HST filters. Because of difficulty in finding guide stars, the nucleus of the galaxy is located in WF3, which has a pixel scale of 0.1’’, corresponding to 8 pc. At least 3 exposures were made for each of the broadband filters, with total exposure times of 1300 seconds in the B filter, 1450 seconds in the R filter, and 1050 seconds in the I filter. The central few pixels were saturated in the I and R images. Four exposures were made for each

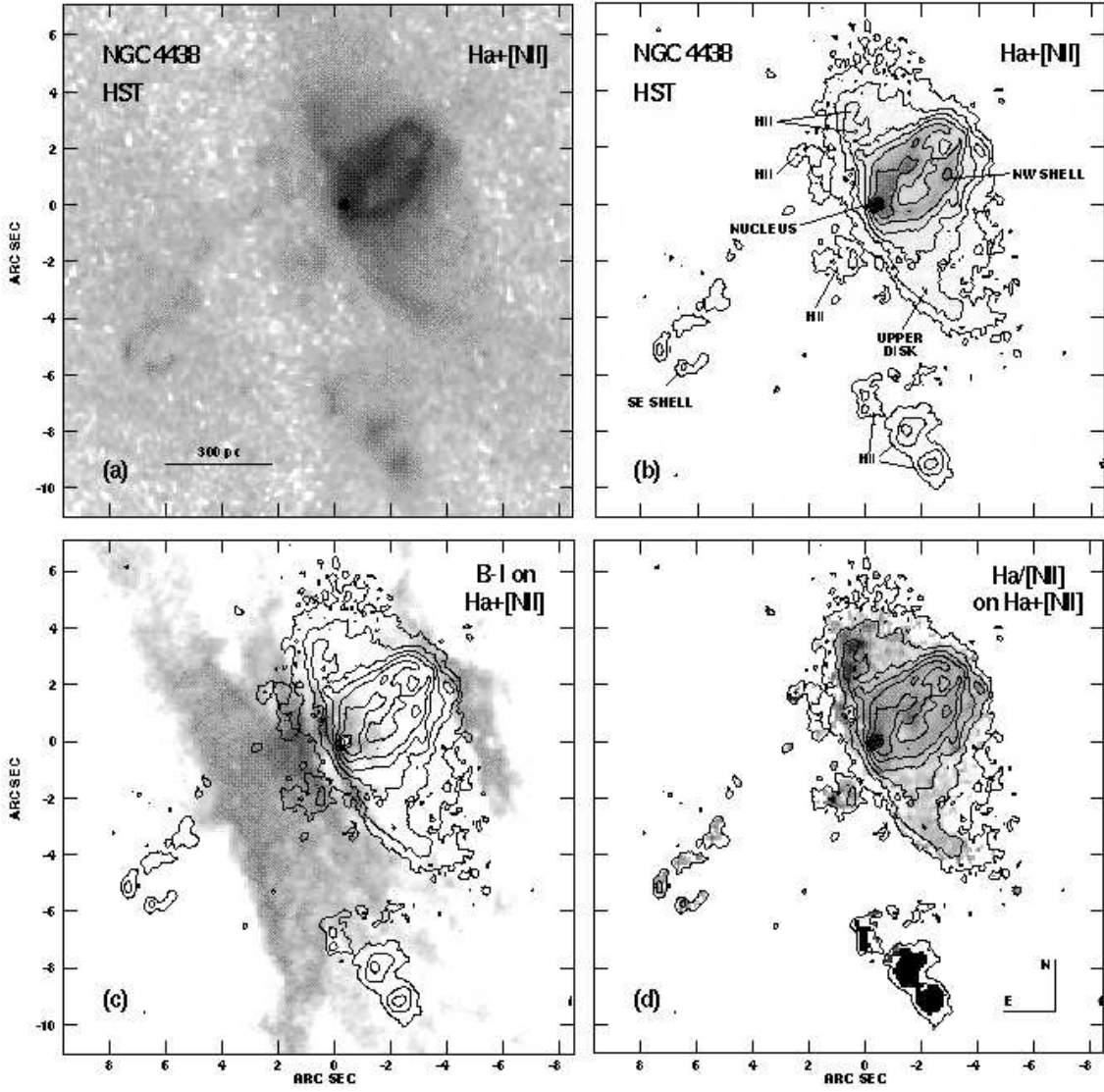


Fig. 1.— a.) Sum of HST $\text{H}\alpha$ and [NII] line images over central $18''$ of NGC 4438. Greyscale stretch is logarithmic. b.) Greyscale and contour maps of $\text{H}\alpha+[\text{NII}]$, with components labelled. c.) F450W-F814W (B-I) greyscale color map superposed on $\text{H}\alpha+[\text{NII}]$ contour map. The gray regions have B-I greater than 1.5, and are largely associated with dust lanes. This shows that part of the SE lobe is likely obscured by dust, and that the line-emitting arc is spatially coincident with the edge of a dust lane. d.) $\text{H}\alpha/[\text{NII}]$ ratio greyscale map superposed on $\text{H}\alpha+[\text{NII}]$ contour map. The lightest grayscale colors correspond to an $\text{H}\alpha/[\text{NII}]$ ratio of 0.3, and the darkest colors correspond to an $\text{H}\alpha/[\text{NII}]$ ratio ≥ 2 . The nucleus has a ratio of 1.6, and the luminous HII complex near the bottom of the frame has ratios between 2-3.

of the narrowband filters, with total exposure times of 5200 seconds for each filter.

All images were processed in the standard HST pipeline using the best available calibration and reference files. The IRAF/STSDAS task gcombine was used to remove cosmic rays and other artifacts from the images and combine the images taken in each filter. The task WFIXUP interpolated over bad pixels, and the task WMOSAIC in IRAF/STSDAS was used to make mosaic images. After cosmic rays were removed, continuum-subtracted H α and [N II] images were made by subtracting scaled versions of the R image from the narrowband images. For the central few pixels which were saturated in the R image, we instead used the unsaturated B image. This introduces an additional error in the central few pixels of the continuum-subtracted H α and [N II] maps, although this error is fairly small because the line emission is relatively strong here. Figure 1a shows the sum of the H α and [N II] images in the central 18''.

3. Results

We use the morphological information shown in the H α +[N II] map of Figure 1a, the H α /[N II] line ratio map shown in Figure 1d, and the broadband B-I color map shown in Figure 1c, to identify 4 types of line emitting components in the central region of NGC 4438: the nuclear source, 2 outflow shells, a few HII regions, and an arc of diffuse gas which likely arises from the upper layers of a dusty gas disk. These components are labelled on the contour plus greyscale H α +[N II] map in Figure 1b. A color-coded combination of all 3 broadband and 2 narrowband images, made by Zolt Levay of STScI, is shown in Figure 2.

3.1. Outflow Shells

The emission line images shown in Figure 1 reveal a double shell morphology straddling a strong compact source which is within 1'' of the nucleus. The 2 shells are quite different, as the northwestern (NW) lobe is bright and compact while the southeastern (SE) lobe is elongated and faint. The NW bubble³ appears as a complete, edge-brightened, roughly elliptical shell, although with significant substructure. The maximum projected radial extent of this shell is 3.8''=290 pc. The nuclear source lies within this elliptical shell and close to

³Keel & Wehrle (1993) spoke of an outflow loop or bubble toward the NW, but this was a much larger and very different feature which Kenney et al. (1995) identify as part of the extended filamentary complex associated with an ISM-ISM or ISM-ICM interaction, and not associated with a nuclear outflow. See Figure 5.

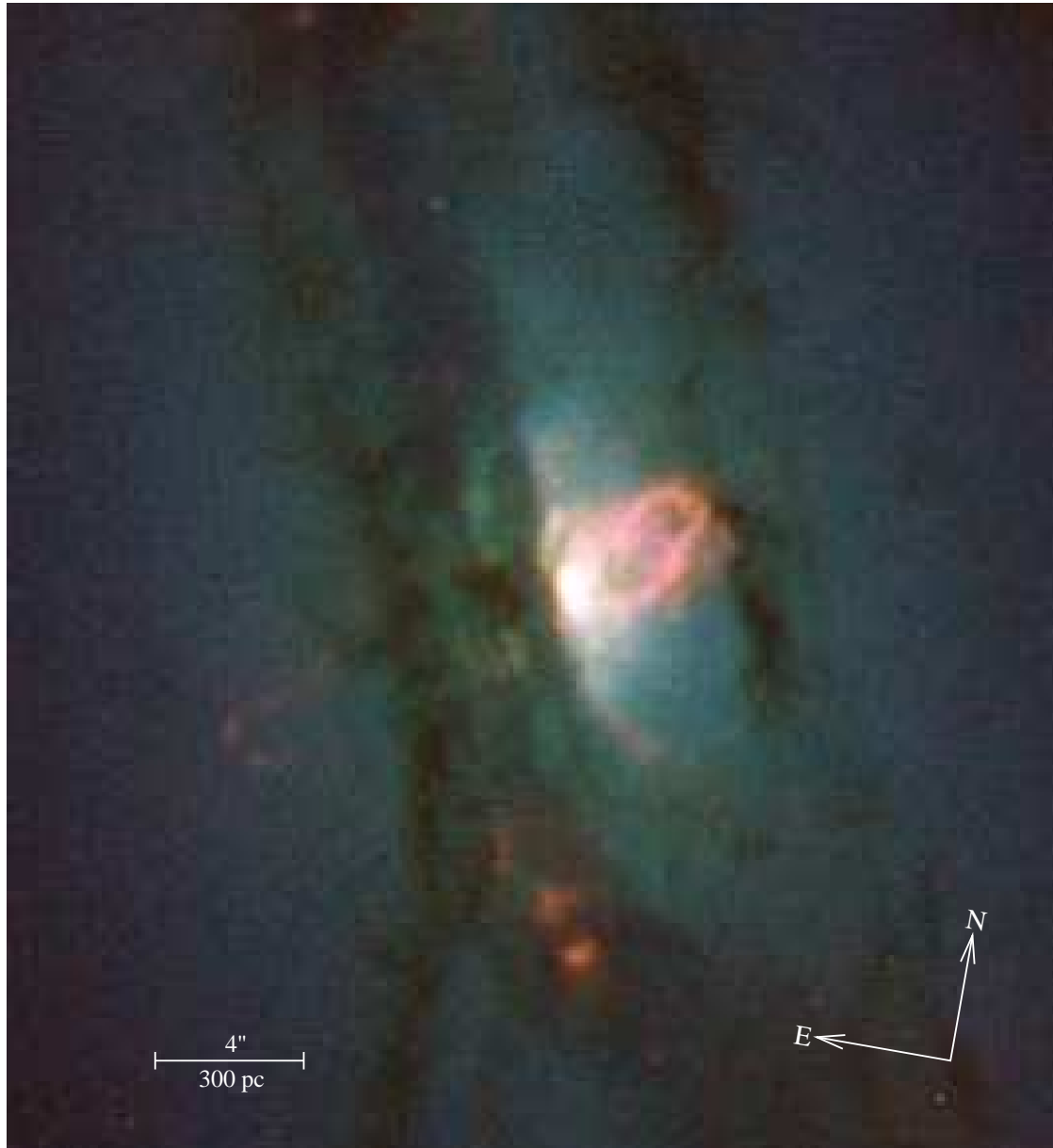


Fig. 2.— Pseudo-color multiband image of central 20'' of NGC 4438, from HST WFPC2. Color coding is: I=red R=green B=blue H α =red/magenta, [NII]=red/orange. The association of arcs of ionized gas with the edges of dust lanes is particularly evident in this image.

the major axis of the ellipse. The nuclear source is thus consistent with being the origin of the energetic outflow presumably responsible for the double bubble morphology.

The position angle of the $\text{H}\alpha + [\text{NII}]$ shells and the radio continuum structure (Hummel & Saikia 1991) is $125 \pm 1^\circ$, which is offset by $6 \pm 2^\circ$ from the minor axis of the galaxy, as determined from the position angle of the major axis of $29 \pm 2^\circ$ for the CO disk and the stellar bulge (Kenney et al. 1995). Thus the bipolar outflow appears to be oriented a bit offset from perpendicular to the stellar disk and to a disturbed circumnuclear ring of molecular gas and dust $\sim 1 \text{ kpc} = 13''$ in radius. The B-I map in Fig. 1c shows a red feature, probably a dust lane, located in projection just above the top of the NW shell, suggesting that a region of enhanced gas density may play a role in determining the spatial extent of the NW shell.

Figure 1d reveals that the $\text{H}\alpha / [\text{NII}]$ line ratios are 0.7-1.0 in the brightest regions of the NW shell, and 0.5-0.7 in the lowest surface brightness regions in the shell interior. It is this bright shell emission which is responsible for the LINER line ratios measured in ground-based spectroscopy (Stauffer 1982; Keel 1983; Ho et al. 1997), and not the nucleus itself (see below). LINERs are a heterogenous class. Some nuclei have LINER line ratios on $< 10 \text{ pc}$ scales, and for such sources the LINER line ratios may arise from photoionization if there is a radial gradient in the gas density (e.g. NGC 4579, Barth et al. 2001). However, in NGC 4438, the shell LINER emission likely arises from shock excitation.

Unlike the NW shell, optical line emission from the SE shell cannot be easily traced to the nucleus. Much of the SE shell is likely obscured by dust. Indeed, the broadband HST images show several dust lanes in this region, and the B-I map in Figures 1c and 2 shows that a major dust lane lies between the nucleus and the visible part of the SE shell. The 2 lobes are also intrinsically quite different. The outer radius of the SE shell is 2.5 times further from the nucleus ($9.5'' = 732 \text{ pc}$) than the corresponding measure for the NW shell, and this cannot be the result of extinction. The opening angle of the SE feature is also significantly less than that of the NW shell.

Moreover, the NW shell is much brighter than the SE shell in the radio continuum as well as in optical line emission (Hummel & Saikia 1991). Figures 3 and 4 show the HST $\text{H}\alpha + [\text{NII}]$ image superposed on the radio continuum maps of Hummel & Saikia (1991). The $1.4''$ resolution 1.4 GHz VLA map in Figure 3 shows a good overall correspondance on large scales between the HST $\text{H}\alpha + [\text{NII}]$ and the radio continuum emission. In particular, the SE radio continuum component is 2.5 longer and 15 times fainter than the western component. Thus the SE and NW components are intrinsically different, and the faintness of the eastern shell in the optical is not entirely due to dust extinction. The $0.4''$ resolution 4.86 GHz VLA map in Figure 4 shows that the luminous NE source has a shell-like morphology with

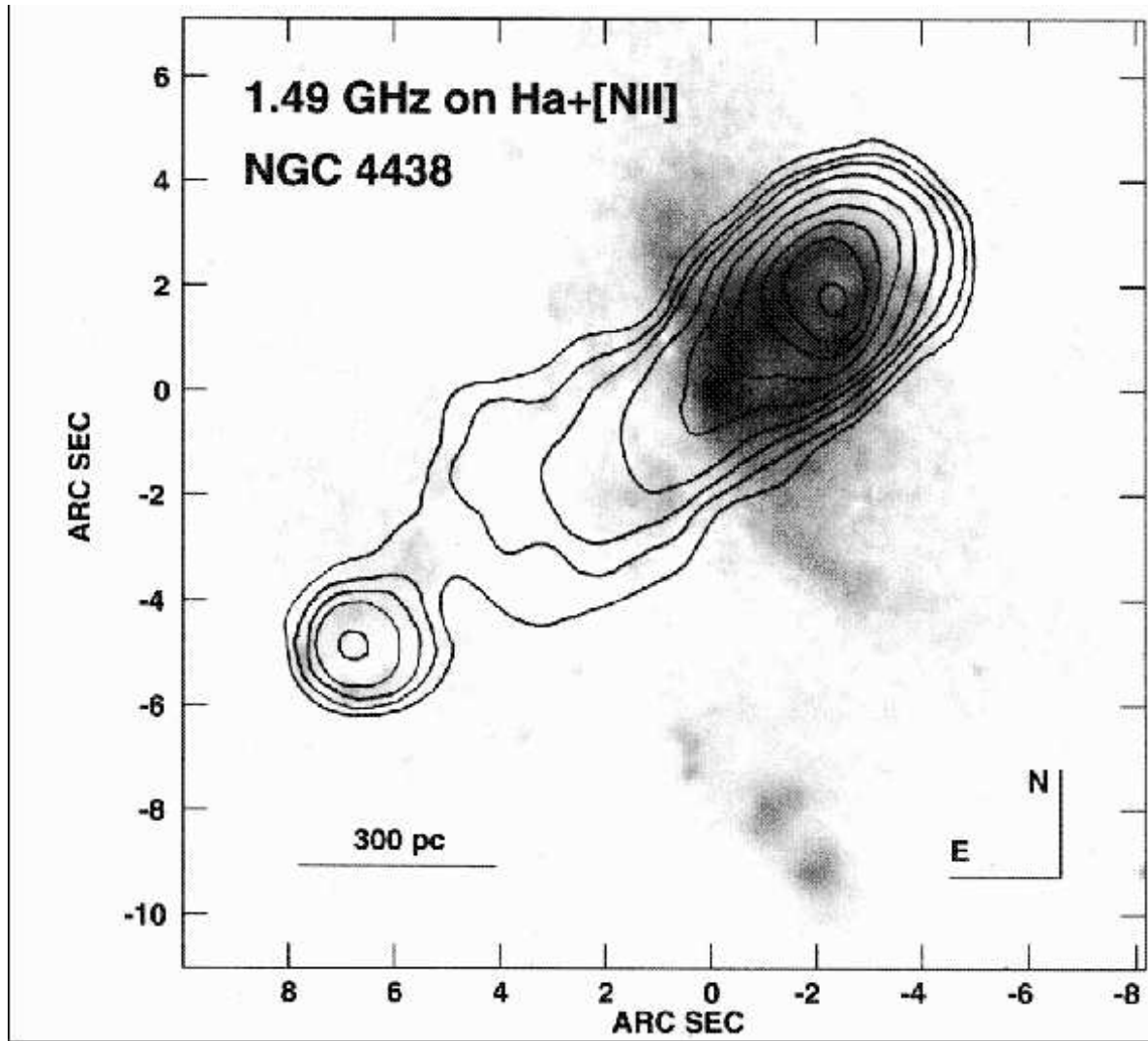


Fig. 3.— HST $\text{H}\alpha + [\text{NII}]$ greyscale image of NGC 4438, superposed on 1.49 GHz radio continuum contour map at 1.2'' resolution from Hummel & Saikia (1991). Note that the NW shell is much brighter and more compact than the SE shell in the non-thermal radio continuum as well as in $\text{H}\alpha + [\text{NII}]$. Note also the enhanced radio continuum emission near the outer ends of the shells, suggesting working surfaces. Greyscale stretch is logarithmic, and contours are 0.2, 0.45, 0.75, 1.25, 2.5, 5, 7.5, 10, 12.5 mJy beam^{-1} .

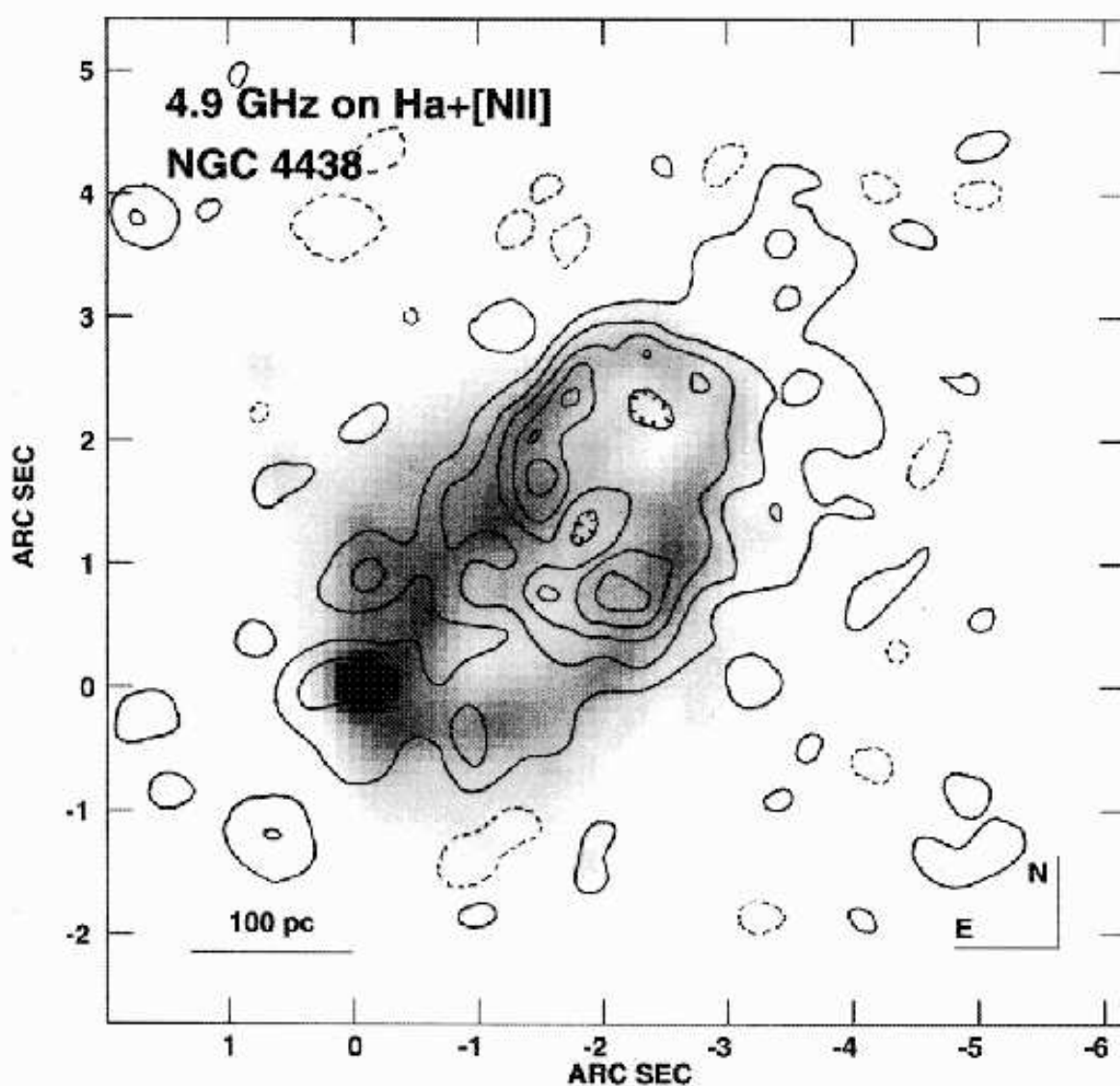


Fig. 4.— HST $\text{H}\alpha + [\text{NII}]$ greyscale image of NGC 4438, superposed on 4.86 GHz radio continuum contour map at 0.4'' resolution from Hummel & Saikia (1991). Note that compared to the $\text{H}\alpha + [\text{NII}]$ emission, the radio continuum emission is relatively stronger inside the shell, and near the outer end of the shell. Note also the presence of radio continuum emission from the nucleus. Greyscale stretch is linear, and contours are -0.1, 0.1, 0.3, 0.5, 0.7, 0.9 mJy beam^{-1} .

sub-structure in the radio continuum as well as in the $\text{H}\alpha + [\text{NII}]$ line. This map also shows a weak radio continuum nuclear source.

Although there is a rough spatial correlation of radio continuum and line emission, there are significant differences. Whereas the $\text{H}\alpha$ and $[\text{NII}]$ surface brightness is similar in the near-nuclear and outer portions of the shell, the outer shell has much stronger radio continuum emission. This suggests working surfaces in which collimated high-velocity nuclear jets or outflows have impacted and shocked the surrounding ISM. As compared to the outer edges of the shell, the interior of the shell has a greater relative brightness in radio continuum than $\text{H}\alpha + [\text{NII}]$, suggesting that the optical line emission only arises at the interface between the outflowing material and the ISM, whereas the radio continuum emission arises from the interior as well as the interface.

This close correspondance between optical narrow line region and radio continuum emitting regions is similar to what is observed in many Seyfert galaxies and other AGN. In many such cases it appears that NLRs form cocoons around the radio jets, probably because shocks driven into the ISM by a jet power the narrow line region. (e.g., Capetti et al. 1999).

3.1.1. Substructure of NW Shell

There is substructure in the NW shell, seen especially in the radio continuum and optical overlay of Figure 4. Morphologically the NW shell seems to have 2 components, and inner and an outer shell, each extending about half the total length. The ratio of radio continuum to $\text{H}\alpha$ surface brightness is much higher in the outer than the inner shell. The ridges of radio continuum curve around and partly cross the interior of the shell, nearly forming a secondary bubble within the larger NW bubble. It appears that the NW bubble may have partially ruptured, and plasma containing most of the relativistic electrons has escaped the initial bubble and formed a secondary bubble. This is similar to NGC 3079, in that the inner part of the outflow has relatively strong $\text{H}\alpha$ emisison, whereas the outer part has relatively strong radio continuum emission (Veilleux et al. 1994).

The mid-axis of the outer shell is not aligned with the mid-axis of the inner shell, but is displaced toward the north. The offset outer shell gives the entire NW shell the appearance of being skewed, but actually the mid-axis of the inner shell lies close to the line connecting the SE shell and the nucleus. It may be that the breakout point of the secondary bubble is not at the apex of the primary bubble, but offset to the N of the apex.

The asymmetry of the NW and SE shells is discussed in §4.3.

3.2. HII Regions

Although there is substantial optical line emission from NGC 4438, the $\text{H}\alpha/\text{[NII]}$ ratio from most if it is less than 1, indicating that photoionization by hot stars is not the dominant source of gas excitation (Keel 1983, Keel & Wehrle 1993). This is true in the central region, as well as globally (Kenney et al. in prep). A modest number of HII regions have been detected in the HST line images. These can be easily identified by their compact morphology, and by relatively high localized $\text{H}\alpha/\text{[NII]}$ line ratios which are between 1.3 and 3.0, as shown in Fig. 1d. The HII regions which we have identified in the central region are indicated in Figure 1b.

Excluding the nucleus itself, there are no large HII regions apparent within $\sim 1''$ of the nucleus, as judged by the low values of the $\text{H}\alpha/\text{[NII]}$ line ratio. While there is some massive star formation occurring in the central few hundred pc of NGC 4438, the star formation rate is quite low. This galaxy is not experiencing a circumnuclear starburst, by which we mean vigorous star forming activity over a region of a few hundred pc, but could be experiencing or have experienced a more compact nuclear starburst.

The brightest star-forming complex in the galaxy is located $8''=600$ pc (projected) south of the nucleus, apparently near the outer edge of the circumnuclear disk of gas and dust, and near the bottom of Figure 1. The measured $\text{H}\alpha+\text{[NII]}$ flux of the entire complex is 2.0×10^{-14} erg s $^{-1}$ cm $^{-2}$, with most of the flux arising from 2 components which are $\sim 1''=77$ pc apart. The corresponding $\text{H}\alpha+\text{[NII]}$ luminosity of 6×10^{38} erg s $^{-1}$ is about an order of magnitude less than 30 Doradus in the LMC, and about two orders of magnitude greater than the Orion Nebula.

3.3. Arc

There is an arc of line emission which passes close to the nucleus and curves toward the west, with a radius of curvature much larger than the western shell. At lower surface brightness levels, the arc appears to fill in toward the west, but cut off more sharply to the east. The eastern boundary coincides with the dust lanes observed in the broadband images, as shown in Figures 1c and 2.

The presence of the arc at the inner edge of the dust lanes suggests that it is ionized by a source near the center of the galaxy, rather than being simply a part of warm diffuse ionized medium which is present in many galaxies (Veilleux, Cecil, & Bland-Hawthorn 1995; Rand 1996). It is likely that there is a dusty gas disk oriented perpendicular to outflow axis, and that the top of this gas disk is illuminated by the central source or the NW shell, causing

the upper layers of the gas disk to be ionized. The HST optical image of Figure 2 suggests that the gas disk has significant structure. It could be that an eastern counterpart exists, but is not visible because of extinction.

The $\text{H}\alpha/\text{[NII]}$ line ratios in this arc are typically 0.5-0.7, except for a few compact spots of with $\text{H}\alpha/\text{[NII]}\simeq 1.3$ along the northern half of this arc, which may be HII regions. The line ratio is lower, typically 0.3-0.5, in the fainter gas to the west of arc. If the arc is ionized by the nuclear source, then the arc may be similar to ionization cones observed in some Seyfert (NGC 1068 – Macchetto et al. 1994) and LINER (NGC 1052 – Pogge et al. 1999) galaxies, although it does not have a straight-edge conical shape, has a very large opening angle, and is relatively faint, distinguishing it from what are usually termed ionization cones.

The radial extent of the optical gas and dust disk is similar to the $13''=1$ kpc radial extent of CO emission detected in OVRO interferometer maps (Kenney et al. 1995). Many of the dust lanes visible near the center of the galaxy appear to lie in an annular ring at radii of $15''$, although there are dust lanes which appear to be non-planar connecting to those in the annular ring.

3.4. Nuclear Source

The brightest line emission arises from a compact but resolved source near the center of the galaxy. This is presumably located at the nucleus, since it is spatially coincident with a bright compact optical continuum source, and is within $1''$ of the centroid of the broadband optical isophotes, which presumably trace the stellar distribution. A more accurate measure is prevented by saturation of the central few pixels in the R and I bands, and by dust. Both the line source and the B-band continuum source are resolved with a full width at half power of $0.32''=25$ pc.

The $\text{H}\alpha/\text{[NII]}$ line ratio of the nuclear source is 1.6 ± 0.4 . This is similar to many of the HII regions, and higher than the values in the outflow shell and surrounding diffuse gas. The central source has an $\text{H}\alpha$ luminosity, without any extinction correction, of 5×10^{38} erg s^{-1} , which is similar to the luminosity of the large HII complex $8''$ south of nucleus and an order of magnitude less than 30 Doradus, but much more compact than either. If the central $\text{H}\alpha$ emission is due to massive star formation, then the present rate of nuclear massive star formation is a minimum of $0.004 \text{ M}_\odot \text{ yr}^{-1}$, since this does not include any extinction correction.

The nucleus appears near the edge of strong dust lanes, as shown in Figures 1c and 2. This implies that the extinction towards the central few hundred pc of NGC 4438 will be

variable, although the nucleus itself may be viewed through relatively less extinction than regions immediately to the SE.

The extinction toward the nuclear source can be roughly approximated from the $\text{H}\alpha/\text{H}\beta$ ratio from ground-based spectra of Keel (1983) or Ho et al. (1997). The spectrum of Ho, obtained with a $2''\times4''$ aperture, has an $\text{H}\alpha/\text{H}\beta$ ratio of 5.67, which compares with the expected ratio of 2.78 for Case B recombination, implying an extinction of $\text{Av}=3.3$ mag, corresponding to 2.6 mag at $\text{H}\alpha$ (Cardelli, Clayton, & Mathis 1989). The NW shell has 7 times the $\text{H}\alpha+[\text{NII}]$ luminosity of the nucleus, so a significant fraction of the flux in ground-based apertures centered on the nucleus comes from the NW shell. Thus the extinction estimate of 2.6 mag is a weighted combination of the extinctions for the nucleus and the NW shell, and the true nuclear extinction could be greater than 2.6 mag, both because of the large aperture in which the $\text{H}\beta$ and $\text{H}\alpha$ lines are measured, and because extinction estimates from optical line ratios generally provide a lower limit on the true extinction. If the extinction at $\text{H}\alpha$ is 2.6 mag, which corresponds to a factor of 11, then the present rate of nuclear massive star formation would be $0.05 \text{ M}_\odot \text{ yr}^{-1}$.

There is a weak radio continuum counterpart to this optical line source (Hummel & Saikia 1991), as shown in Fig 4. The nuclear flux density estimated from the map of Hummel & Saikia (1991) is 1.5 ± 0.3 mJy at 4.86 GHz, which corresponds to a power of $5.0\times10^{19} \text{ W Hz}^{-1}$. The spectral index of the nucleus is uncertain, since it is faint and unresolved in the 1.4 GHz map of Hummel & Saikia (1991), as shown in Figure 3. The radio continuum emission at 4.86 GHz from star forming regions in galaxies is a mixture of thermal and non-thermal emission. If the spectral index of non-thermal component of the nuclear source has the typical value of 0.8, then at 4.86 GHz about 3/4 of the flux is non-thermal, and 1/4 is thermal (Condon 1992). If this radio continuum power is all due to star formation, then the steady-state total star formation rate is about $0.1 \text{ M}_\odot \text{ yr}^{-1}$, according to the relations given in Condon (1992). This yields an upper limit of a factor of 24, or 3.4 magnitudes, on the extinction at $\text{H}\alpha$ toward the nuclear source, if the radio continuum emission is dominated by star formation. Given the uncertainties, this agrees well with the $\text{H}\alpha$ -based estimate of the nuclear star formation rate.

If the nuclear radio continuum and $\text{H}\alpha$ emission are powered predominantly by something other than star formation, then the radio continuum emission cannot be used to estimate the extinction at $\text{H}\alpha$, although the upper limit on the the nuclear star formation rate would still hold.

4. Discussion

4.1. Energetics of the Shells

In order to obtain some kinematic information on the shells, we have reanalyzed the ground-based optical slit spectra of NGC 4438 described by Kenney et al. (1995) and Rubin et al. (1999), which was obtained with the Kitt Peak 4m telescope. The spectrum taken at a position angle of 104° , is the closest to the shell position angle of 125° , and passes through the western edge of the NW shell. Given the slit orientation and the limited spatial resolution ($2''$) of this ground-based data, we are not able to extract a useful limit on the velocity gradient across the shell, but can provide some linewidth information. The FWHMs of the brighter of the [NII] and [SII] lines are measured in $2''$ apertures to be 408 km s^{-1} at the nucleus, $\sim 200 \text{ km s}^{-1}$ at $5\text{-}10''$ from the nucleus (well beyond the shell), and 290 km s^{-1} at $2\pm1''$ from the nucleus, where the slit covers the the western edge of the NW shell. This linewidth would contain contributions from both bulk and turbulent motions, but could greatly underestimate the bulk outflow motions. The true internal velocities could be significantly higher, since the maximum velocities are likely projected close to the plane of the sky, and since the largest line-of-sight velocities are probably occur near the bubble mid-axis (as in NGC 3079, Veilleux et al. 1994), and our ground-based spectrum misses the mid-axis of NGC 4438’s bubble. We nonetheless adopt a reasonable lower limit on the internal motions of the brightest optical line emitting gas in the NW shell of 300 km s^{-1} .

The [SII] doublet ratio $\lambda 6716/\lambda 6731$ at the western edge of the NW shell is measured from our Kitt Peak 4m spectrum to be 1.08 ± 0.01 , which corresponds to an electron density of 420 cm^{-3} , for an electron temperature of 10^4 K (Osterbrock 1989).

The $\text{H}\alpha$ luminosity of the NW shell is $3.4\times10^{39} \text{ erg s}^{-1}$, assuming no extinction correction, which corresponds to a mass of ionized gas of $3.5\times10^4 \text{ M}_\odot$, assuming an electron density of 420 cm^{-3} (Osterbrock 1989; Veilleux, Shopbell & Miller 2001). Assuming the same mass for the SE shell, the total ionized gas mass of $7\times10^4 \text{ M}_\odot$ for NGC 4438 would be somewhat less than, although similar to, the ionized gas masses in the outflows of M82 ($2\times10^5 \text{ M}_\odot$) and NGC 3079 ($1\times10^5 \text{ M}_\odot$) (Veilleux et al. 1994).

This ionized gas mass of the NW shell has an associated kinetic energy of $6\times10^{52} \text{ erg}$, assuming a velocity of 300 km s^{-1} . Assuming the same KE for the SE shell, the KE for the 2 shells would be $1.2\times10^{53} \text{ erg}$. This is a lower limit on the KE, since it does not include atomic, molecular, or hotter ionized gas components, does not include any extinction correction, and is based on a lower limit to the internal velocities. This KE is similar to the that associated with the ionized gas in the outflow in M82 ($2\times10^{53} \text{ erg}$), although significantly lower than that in NGC 3079 ($2\times10^{54} \text{ erg}$) (Veilleux et al. 1994). The mass and kinetic energy associated

with the ionized gas in the outflow of NGC 4438 is comparable to that in M82, despite the fact that the central star formation rate in NGC 4438 appears to be roughly one order of magnitude lower.

4.2. A Starburst or AGN Origin?

What is the nature of the nuclear energy source driving the outflows?

The lower limit on the kinetic energy in the shells of 10^{53} erg is equivalent to about 100 supernovae. Assuming a Salpeter initial mass function and an upper mass cutoff of $100 M_{\odot}$, this would correspond to a total mass of more than $10^4 M_{\odot}$ in stars formed within the last 10^6 yr (Elson et al. 1989), and an average star formation rate of $0.01 M_{\odot} \text{ yr}^{-1}$. Since the base of the outflow seems to be quite narrow, this activity would need to have occurred within the central $1''=77$ pc. The upper limit on the present rate of massive star formation in the nucleus, as estimated from the extinction-corrected nuclear H α emission or the nuclear radio continuum emission, is $0.05\text{--}0.1 M_{\odot} \text{ yr}^{-1}$ (§3.4).

Thus a starburst origin for the shells is energetically plausible, given the present estimate of the kinetic energy in the shells. Moreover, the H α /N[II] ratio of the nucleus is consistent with that of an HII region. Although no known starburst outflow has the large degree of collimation of the SE shell, or strongly enhanced radio continuum emission at the outer ends of the shells, it might be that the outflow from the formation of a compact nuclear star cluster could be sufficiently collimated to produce the observed working surfaces.

The outflow axis is shifted by $\sim 6^\circ$ from the apparent minor axis of the 100-1000 pc scale CO disk. This is not strong evidence for either the starburst or AGN scenario. A large misalignment would indicate an AGN jet, whereas alignment would be consistent with an extended starburst. Given the disturbed morphology of the galaxy, we do not attribute much significance to the relatively small offset.

While some properties of the outflow are consistent with a nuclear starburst outflow, others are more indicative of jets associated with nuclear black holes. The low level of star formation in the central 100 pc, the collimation of the SE shell, the enhanced radio continuum brightness at the outer ends of the shells, and the broad line component, are all suggestive of a nuclear power source more exotic than star formation.

The broad line component with $\text{FWHM}=2050 \text{ km s}^{-1}$ reported by Ho et al (1997) is suggestive of a “true AGN”, and might arise from an accretion disk. However, lines this wide can also occur in outflowing gas. While most outflows associated with superbubbles

have velocities of a few hundred km s⁻¹ (Heckman, Armus, & Miley 1990), the starburst-plus-AGN galaxy NGC 3079 has extranuclear H α velocities of 2000 km s⁻¹ in the outflowing gas (Veilleux et al. 1994). So the existence of a moderately broad component to the H α line in NGC 4438 does not by itself distinguish between an AGN and starburst as the driver of the outflow.

A possible problem with the AGN jet scenario is that no jet has been detected. Most of the radio continuum emission in Figs. 3 and 4 arises from the edges and ends of the shells. While no jet has been detected, there are suggestions that some Seyfert jets are sub-relativistic and weak emitters of synchrotron radiation on 100 pc scales (Bicknell et al. 1998). Much of the energy in Seyfert jets may be associated with thermal rather than relativistic plasma.

Since NGC 4438 has a large bulge with a luminosity of 10^{10} L $_{\odot}$, a large nuclear black hole might be expected. There is no published stellar velocity dispersion for NGC 4438, but the rough correlation between bulge luminosity and black hole mass shown by Ferrarese & Merritt (2000) or Gebhardt et al. (2000) suggests a black hole mass of $\sim 5 \times 10^7$ M $_{\odot}$ for NGC 4438. Such a large black hole mass should produce a kinetic signature detectable with HST resolution.

The nuclear region of NGC 4438 hosts an x-ray source detected by both the Einstein and ROSAT satellites. The Einstein High Resolution Imager measured a luminosity from 0.1-2 keV of L_x = 3×10^{39} erg s⁻¹ (Kotanyi, van Gorkom & Ekers 1983), whereas the ROSAT High Resolution Imager measured a significantly higher luminosity from 0.1-2.4 keV of L_x = 1.3×10^{40} erg s⁻¹ (Roberts & Warwick 2000). The nuclear source is unresolved by both the Einstein and the ROSAT HRIs, which have resolutions of $\simeq 10''$, so it is unclear how much of this emission arises from the nucleus and how much from the outflows. Even if all of this emission arises from the nuclear source, the observed x-ray luminosity (even with the lower Einstein value) is significantly below the Eddington luminosity for a black hole mass of 5×10^7 M $_{\odot}$, suggesting accretion onto the black hole at a sub-Eddington rate. This appears to be the situation for most nearby galaxies (Roberts & Warwick 2000), and is consistent with the accretion rates suggested for advection-dominated accretion flows (ADAFs – Narayan & Yi 1995; Fabian & Rees 1995).

NGC 4438 has also been detected in x-rays by the ASCA satellite, which provides information about the x-ray spectrum. Terashima, Ho, & Ptak (2000) found a reasonably good correlation between the hard (2-10 keV) ASCA x-ray luminosity and the H α luminosity in the central $2'' \times 4''$ for LINER 1 galaxies, defined to be those LINERs which contain a broad component to the H α line. The correlation is poor for LINER 2 galaxies. This provides evidence that the hard x-ray emission from an AGN is the source of ionization for

the optical line emission observed near the nuclei of most LINER 1 galaxies, and that some other mechanism is likely for LINER 2 galaxies.

The only LINER 1 galaxy in their sample which deviated strongly from this correlation was NGC 4438, which had a ratio of hard x-ray to H α luminosity one to two orders of magnitude lower than the rest. This could be partly, but not entirely, due to strong H α emission from the NW outflow shell in NGC 4438, which contributes significantly to the flux in a $2'' \times 4''$ aperture. The ionized gas associated with the shell is likely shock excited due to the outflow. If one compares the hard x-ray luminosity with H α luminosity from the nuclear source only (about half the total in the central $2'' \times 4''$), then NGC 4438 is somewhat closer to the other LINER 1's, but still has a significantly lower ratio of L_x/L_{H α} . This suggests that NGC 4438 is a significantly different nuclear source from most LINER 1's, and that the broad H α component might be gas in the outflow, and not a true broad line component (e.g., emission from an accretion disk).

4.3. The Asymmetries of the Outflow Shells

Some properties of the nuclear emission regions may be due to peculiarities in the circumnuclear environment caused by the interaction(s) experienced by NGC 4438. We would not be the first to speculate that an interaction has increased the flow of gas into the nucleus, fueling a nuclear starburst or feeding a central black hole, although it is difficult to establish any direct causal connections between nuclear fueling and the large-scale environment for any one particular galaxy. On the other hand, a case can be made that the asymmetries in the outflow shells are associated with the global disturbance to NGC 4438.

The differences in luminosity, length, and opening angle between the two shells are among the most striking features of the nuclear outflow in NGC 4438. The SE shell is 2.5 times longer, 15 times less luminous in the radio continuum, and has an opening angle much narrower than the NW shell. These 3 differences can all be explained in principle by jet material running into an ISM which is denser on the NW side of the disk than the SE. Even if the energy injected is the same on both sides, a larger fraction of the energy is dissipated on the NE side as the outflowing material is significantly decelerated, resulting in more radiation. Similarly, the impedance associated with a higher ISM density has been considered at least part of the reason why jets in spiral galaxies tend to have wider opening angles and smaller lengths than those in ellipticals (Elmouttie et al. 1998). The higher luminosity together with the compact morphology of the NW shell suggest that it is at the stage of superbubble evolution in which radiative losses are dynamically important (e.g., Weaver et al. 1977; Ostriker & McKee 1988). On the other hand, the SE shell is likely to

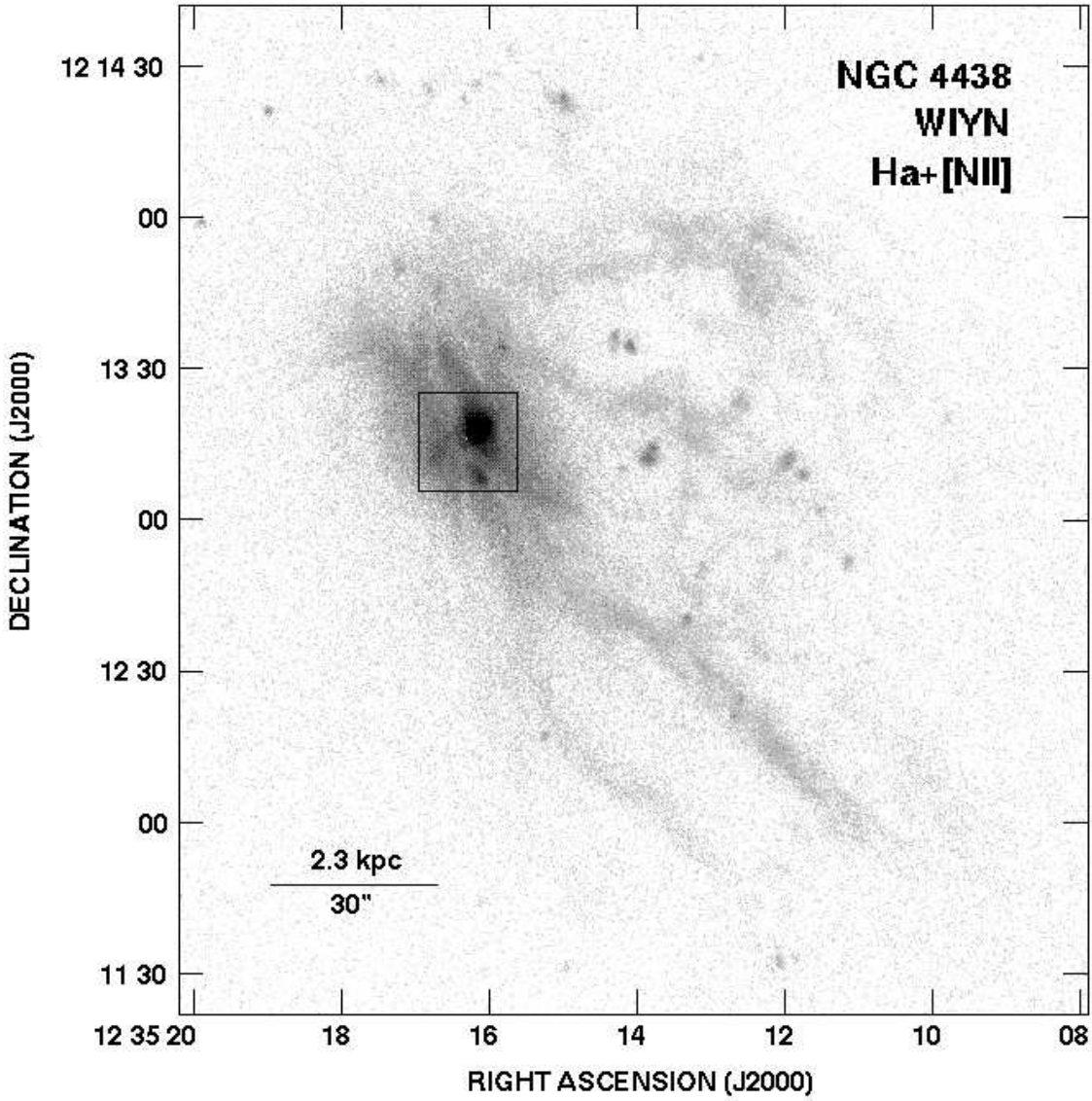


Fig. 5.— WIYN $\text{H}\alpha$ +[NII] image of NGC 4438, with resolution of $1''$ and $180'' \times 200''$ field of view, shown with a logarithmic stretch. This image shows the larger scale environment into which the nuclear outflow is propagating. The inset box outlines the region shown in Figures 1 and 3. The nucleus plus NW shell, the SE shell, the strong dust lane crossing the SE shell, and the HII complex $8''$ of the nucleus can all be seen within the inset region. In addition, 2 larger-scale ionized gas components are apparent – a diffuse component of $\sim 30'' \times 60''$ extent, and a one-sided filamentary nebula extending out $120''$ to the NW. There are HII regions located within the one-sided filamentary nebula, although only a small fraction of the emission arises from HII regions. Note that the large scale ISM asymmetry in NGC 4438, with emission on the NW side much stronger than on the SE side, is the same as that observed for the nuclear outflow shells.

be in an earlier, free-expanding or adiabatic phase.

A systematic difference in the circumnuclear ISM density on the 2 sides of the disk seems plausible, since the ISM of NGC 4438 shows this asymmetry on larger scales. Much of the HI, CO, H α , radio continuum, and x-ray emission are strongly displaced to the west of the stellar disk (Kotanyi et al. 1983; Combes et al. 1988; Cayatte et al. 1990; Kenney et al. 1995), presumably due to an interaction in the cluster. Figure 5 shows a ground-based H α +[NII] image from the WIYN telescope, over a $180'' \times 200''$ field of view, with $1''$ resolution (Kenney et al. in prep). This shows the ISM environment into which the nuclear outflow is propagating. Inside the box in the center, which outlines the $18''$ field of view shown in Figures 1 and 3, the nucleus plus NW shell, the SE shell, the dust lane crossing the SE shell, and the HII complex $8''$ of the nucleus can all be seen. In addition, 2 larger-scale ionized gas components are apparent – a diffuse component of $\sim 30'' \times 60''$ extent, and a one-sided filamentary nebula extending out $120''$ to the NW. There are HII regions located within the one-sided filamentary nebula, although only a small fraction of the emission arises from HII regions. Note that the large scale ISM asymmetry in NGC 4438, with emission on the NW side much stronger than on the SE side, is the same as that observed for the nuclear outflow shells.

If this same asymmetry extends down to scales of 10 pc, this could explain why the NW shell is so much brighter and shorter than the SE shell. The gas, which may be slowly infalling back into NGC 4438 after a galaxy-galaxy collision (Kenney et al. 1995), may not fall much further than the disk midplane, since it will collide with the gas already in the disk. The strong emission of the NW shell may arise because the ISM above the disk plane is unusually dense, due to the disturbance experienced by NGC 4438, resulting in a stronger interaction between the outflow and the ambient ISM.

We have examined the [SII] $\lambda 6716/\lambda 6731$ doublet ratio from the ground-based optical spectrum cited above (along PA=104°) in order to see whether there is any difference in ionized gas density of the 2 sides of the galaxy. The [SII] ratios measured $6 \pm 1''$ from the nucleus on both sides of the galaxy do show a significant difference. On the NW side, a few arcseconds beyond the NW shell, the [SII] ratio is 1.07 ± 0.02 , which corresponds to an electron density of 450 cm^{-3} , whereas at the same distance from the galaxy center toward the SE, the [SII] ratio is 1.15 ± 0.02 , which corresponds to a lower electron density of 310 cm^{-3} . This provides evidence that the gas density on the 2 sides of the galaxy disk may indeed be different.

4.4. Other Galaxies with Similar Outflow Morphologies

Many active galaxies contain one-sided or bipolar nuclear narrow line emission features, including jets, shells, bubbles or ionization cones, which extend 100's to 1000's of pc's (e.g., Wilson et al. 1993; Wilson & Tsvetanov 1994; Macchetto et al. 1994; Baum & Heckman 1989; Baum et al. 1993; Lenhert & Heckman 1996; Falcke et al. 1998). The morphologies vary widely, even among galaxies with a given nuclear classification. For example, Pogge et al. (1999) have recently imaged the line emission in 14 LINERs with HST, and found a variety of morphologies, few of them well-ordered, and none of them much like NGC 4438. Those galaxies whose nuclear regions most closely resemble the one in NGC 4438 are those with closed shells, double bubble, or figure-8 shaped morphologies, in narrow emission lines and/or the radio continuum. There are such features in both Seyfert and starburst/LINER galaxies, and it is not always clear whether they are formed by AGN jets or starburst winds since both can form bubbles.

The Seyfert 2 galaxy NGC 2992 exhibits a figure-8 shaped morphology in the radio continuum (Ulvestad & Wilson 1984), although the narrow line morphology is dominated by an ionization bi-cone apparently unrelated to the radio continuum lobes (Allen et al. 1999). The ionization from the strong Seyfert nucleus of this galaxy may overwhelm that from the edge-brightened bubbles of radio plasma producing the radio lobes. Although nuclear jets may be responsible for blowing the nuclear bubbles, there is no strong enhancement in radio emission at the outer ends of the lobes, and therefore no evidence of working surfaces in NGC 2992, in contrast to both NGC 4438 and the Seyfert 2 galaxy NGC 3393. NGC 3393 contains a narrow-line region dominated by S-shaped arms which border a linear, triple-lobed radio source (Cooke et al. 2000). The origin of the S-shaped emission line region is not clear, but might result from either an incomplete bipolar bubble or precessing jets. The strongest radio emission associated with the optical arms does not trace the optical arms, but arises from smaller regions which are spatially coincident with part of the optical arms. These are presumably working surfaces where a jet is strongly interacting with the surrounding ISM.

The starburst/LINER galaxies NGC 2782 (Jogee et al. 1998, 1999) and NGC 3079 (Ford et al. 1986; Veilleux et al. 1994; Cecil et al. 1999; Veilleux 2000) exhibit partially closed shell morphologies in emission lines and the radio continuum. The optical and radio shells are roughly spatially coincident in NGC 2782 (Jogee et al. 1998) whereas in NGC 3079 the radio shell is significantly more extended than the optical shell (Ford et al. 1986). This suggests that NGC 2782 may be in a pre-blowout phase of starburst superwind evolution (Chevalier & Clegg 1985; Tomisaka & Ikeuchi 1988; Heckman et al. 1990), and that NGC 3079 may be in an early blowout phase. While the role of AGN in these 2 galaxies cannot be discounted, both of these galaxies contain nuclear starbursts, and neither exhibits a strong enhancement

in radio continuum at the outer ends of their lobes. These properties distinguish them from NGC 4438.

Further exploration into the differences between these galaxies may be helpful in general for distinguishing between the outflows of nuclear star formation and supermassive black holes.

5. Future Work

Ultimately we wish to know nature of the nuclear source and whether the outflow is driven by AGN or starburst. The present study has not given definite answers for these questions, and future studies will help provide the answers.

High spatial resolution optical or infrared spectroscopy of the nucleus could show the spatial distribution of the 2000 km s^{-1} broad line component, revealing whether it originates in the outflowing gas or is a true AGN broad line component. It could also show whether there is a very broad line component on sub-arcsecond scales possibly arising from an accretion disk, as in the Virgo LINER NGC 4579 (Barth et al. 2001). Studies of the stellar kinematics from absorption lines can constrain the mass of a central black hole and show whether the outflow originates from the dynamical center of the galaxy. IR imaging and spectroscopy can provide better extinction estimates, further revealing the true nature of the nucleus, and yielding new information on the spatial extent and intensity of the central star formation activity.

High resolution x-ray observations (Chandra) can show how much of the central $10''$ Einstein and ROSAT x-ray source is associated with the nucleus, and how much with the outflow. The x-ray spectrum of the nuclear source can reveal the true nature of the nucleus, whereas that of the outflow can reveal whether the hot gas has sufficient energy to be dynamically important for the evolution of the bubble. In M82 the high temperature ($4 \times 10^7 \text{ K}$) thermal x-rays may contain enough pressure to drive the outflow (Griffiths et al. 2000).

High resolution molecular gas (e.g. CO) observations may be important for learning the energy budget of bubbles, since molecular gas may be participating in the outflow, and could be carrying a significant amount of kinetic energy. Most of the kinetic energy associated with a starburst superbubble in M82 appears to be in the form of molecular rather than ionized gas (Matsushita et al. 2000), and it will be interesting to learn whether the bubbles in NGC 4438 are similar.

We find it remarkable that there is a such a striking outflow from a nucleus without

a very luminous starburst or AGN, and think followup studies of NGC 4438 and similar galaxies are important because of the possible implications for the deposition of matter and energy into galactic haloes and the intergalactic medium.

6. Acknowledgements

We thank the referee Sylvain Veilleux for helpful comments which resulted in an improved paper, and Simon Cassasus for analyzing the ground-based spectra, and for his interest. We are also grateful to Andrew Baker, Stefi Baum, Paolo Coppi, Carol Mundell, Chris O'Dea, Megan Urry, and Andrew Wilson for helpful exchanges, and Zolt Levay for producing the beautiful color images. This work has been supported by Space Telescope grant GO-06791.

REFERENCES

Allen, M. G., Dopita, M. A., Tsvetanov, Z. I., & Sutherland, R. S. 1999, *ApJ* 511, 686
Barth, A. J., Ho, L. C., Filippenko, A. V., Rix, H.-W., & Sargent, W. L. W. 2001, *ApJ*, 546, 205
Baum, S. A., & Heckman 1989, *ApJ*, 336, 702
Baum, S. A., O'Dea, C. P., Dallacassa, D., de Bruyn, A. G., & Pedlar, A. 1993, *ApJ*, 419, 553
Bicknell, G. V., Dopita, M. A., Tsvetanov, Z. I., & Sutherland, R. S. 1998, *ApJ*, 495, 680
Capetti, A., Axon, D. J., Macchetto, F. D., Marconi, A., & Winge, C. 1999, *ApJ*, 516, 187
Cardelli, J. A., Clayton, G. C., & Mathis, J. S. 1989, *ApJ*, 345, 245
Cayatte, V., van Gorkom, J. H., Balkowski, C., & Kotanyi, C. 1990, *AJ*, 100, 64
Cecil, G. 1988, *ApJ*, 329, 38
Cecil, G., Veilleux, S., Filippenko, A. V., & Bland-Hawthorn, J. 1999, *BAAS*, 195, 0808C
Combes, F., Dupraz, C., Casoli, F., & Pagani, L. 1988, *AA*, 203, L9
Condon, J. J. 1992, *ARAA*, 30, 575
Cooke, A. J., Baldwin, J. A., Ferland, G. J., Netzer, H., & Wilson, A. S. 2000, *ApJS*, 129, 517
Elmouttie, M., Haynes, R. F., Jones, K. L., Sadler, E. M., & Ehle, M. 1998, *MNRAS*, 297, 1202

Elson, R. A., Fall, S. M., & Freeman, K. C. 1989, 336, 734

Fabian, A. C., & Rees, M. J. 1995, MNRAS, 277, 55

Falcke, H., Wilson, A. S., & Simpson, C. 1998, ApJ, 502, 199

Ferrarese, L., & Merritt, D. 2000, ApJ, 539, L9

Filippenko, A. V. 1996, in the Physics of LINERs in View of Recent Observations, ed. M. Eracleous et al. (San Francisco: ASP), 17

Ford, H. C., Dahari, O., Jacoby, G. H., Crane, P. C., & Ciardullo, R. 1986, ApJ, 311, L7

Freedman, W. L. et al. 1994, Nature, 371, 757

Gebhardt, K. et al. 2000, ApJ, 539, L13

Heckman, T. 1980 AA, 87, 152

Heckman, T. M., Armus, L., & Miley, G. K. 1990, ApJS, 574, 833

Heckman, T. M., Baum, S. A., van Breugel, W. J. M., & McCarthy, P. 1989, ApJ, 338, 48

Ho, L. C. 1999, ApJ, 510, 631

Ho, L. C., Filippenko, A. V., & Sargent, W. L. W. 1997, ApJS, 112, 315

Hummel, E., & Saikia, D. J., 1991, AA, 249, 43

Jacoby, G. H. et al. 1992, PASP, 104, 599

Jogee, S., Kenney, J. D. P., & Smith, B. J. 1998, ApJL, 494, L185.

Jogee, S., Kenney, J. D. P., & Smith, B. J. 1999, ApJ, 526, 665.

Katsiyannis, A. C., Kemp, S. N., Berry, D. S., & Meaburn, J. 1998, AAS, 133, 397

Keel, W. C. 1983, ApJ, 269, 466

Keel, W. C., & Wehrle, A. E. 1993, AJ, 106, 236

Kenney, J. D. P., Rubin, V. C., Planesas, P., & Young, J. S. 1995, ApJ, 438, 135

Kennicutt, R. C., Jr., 1983, ApJ, 272, 54.

Kennicutt, R. C., Jr., Edgar, B. K., & Hodge, P. W. 1989, ApJ, 337, 761.

Kormendy, J., & Richstone, D., 1995 ARAA, 38, 581

Kotanyi, C. G., van Gorkom, J. H., & Ekers, R. 1983, ApJ, 273, L7

Lenhert, M. D., & Heckman, T. M. 1996, ApJ 462, 651

Macchetto, F., Capetti, A., Sparks, W. B., Axon, D. J., & Boksenberg, A. 1994, ApJ, 435, L15

Magorrian, J. et al. 1998, AJ, 115, 2285.

Moore, B., Katz, N., Lake, G., Dressler, A., & Oemler, A., Jr. 1996, *Nature*, 379, 613

Narayan, R., & Yi, I. 1995, *ApJ*, 452, 710

Osterbrock, D. E., 1989, *Astrophysics of Gaseous Nebulae and Active Galactic Nuclei*, (Mill Valley, CA: University Science Books)

Ostriker, D. E., & McKee, C. F. 1988, *Rev. Mod. Phys.*, 60, 1

Pogge, R. W., Maoz, D., Ho, L. C., & Eracleous, M. 2000, *ApJ*, 532, 323

Rand, R. J. 1996, *ApJ*, 462, 712

Roberts, T. P., & and Warwick, R. S. 2000, *MNRAS*, 315, 98

Rubin, V. C., Waterman, A. W., & Kenney, J. D. P. 1999, *AJ*, 118, 236.

Stauffer, J. R. 1982, *ApJ*, 262, 66

Terashima, Y., Ho, L. C., & Ptak, A. F. 2000, 539, 161

Tomisaka, K., & Ikeuchi, S. 1988, *ApJ*, 330, 695.

Ulvestad, J. S., & Wilson, A. S. 1984, *ApJ*, 285, 439.

Ulvestad, J. S., Wilson, A. S., & Sramek, R. A. 1981, *ApJ*, 247, 419.

Veilleux, S., 2000, *ASP Conf. Series*, Vol. 195, ed. W. van Breugel & J. Bland-Hawthorn, 277

Veilleux, S., Cecil, G., Bland-Hawthorn, J., Tully, R. B., Filippenko, A. V., & Sargent, W. L. W., 1994, *ApJ* 433, 48

Veilleux, S., Shopbell, P. L., & Miller, S. T. 2001, *AJ*, 121, 198

Veilleux, S., Cecil, G., & Bland-Hawthorn, J., 1995, *ApJ*, 445, 152

Weaver, R., et al. 1977, *ApJ*, 218, 377

Wilson, A. S., & Tsvetanov, Z. I. 1994, *AJ*, 107, 1227

Wilson, A. S., Braatz, J. A., Heckman, T. H., Krolik, J. H., & Miley, G. K. 1993, *ApJ*, 419, L61